

Nathan Hugh Barr

March 8, 2019

Abstract

Abstract here

Contents

1	Introduction	3
1.1	Research Question	4
1.2	Structure of this thesis	4
2	Theory	6
2.1	Electromagnetic Radiation	6
2.2	Refractive index	7
2.3	Reflectance and Transmittance	8
2.4	Fresnel equations for the ambient-substrate model	9
2.5	Fresnel equations for the ambient-thin film-substrate model	11
2.6	Fresnel equations for a multilayer model	14
3	Experimental method	17
3.1	Polymers	17
3.2	Polymers used in Solvent Vapour Annealing	19
3.2.1	Homopolymer Chemistry	19
3.3	Polymer Considerations	20
3.3.1	Relevant values	20
3.4	Spin Coating thin films	20
3.5	Spectrometer Setup	21
3.6	Reflectance measurements in the NanoCalc spectrometer	21
3.7	Reflectance measurement protocol	24
3.7.1	Without Optics	24
3.7.2	With Optics	25
3.8	MATLAB® result fitting	25
3.9	Bronkhorst mass flow meters	25
3.10	Solvent Vapour Annealing Process	26
4	Analysis	28
4.1	Nano-Calc Simulated Reflectance Curves	28

4.2 Day study	28
4.3 Ambient study	28
4.4 Polystyrene	28
4.5 Polyisoprene	28
4.6 Polystyrene-b-polyisoprene	28
5 Bibliography	29

Chapter 1

Introduction

In December 2017 and May 2018, I was asked to partake in Grazing-incidence small-angle scattering(GISAXS) experiments investigating the structure of thin films at The Cornell High Energy Synchrotron Source (CHESS). A thin film is a thin layer of polymer deposited onto a wafer, in this case a silicon wafer. The experiments were conducted with the aim of understanding the reorganisation of star-block polymers on a silicon wafer when exposed to vapour annealing. GISAXS maps were used to study how the star-block polymers arranged themselves when the volume of the polymer increased. GISAXS maps gives the researcher a snapshot of the polymers structure at that point in time. The GISAXS maps can be used to calculate the thickness of the polymer, this is not a trivial since it involves fitting a model[explain a bit more], it is also done post experiment and is time consuming.

This leads to the experimental method called Spectroscopic Reflectometry, and the meaning of these two words gives insight into the nature of the method. Spectroscopic is a study of the interaction between electromagnetic radiation and matter [1] and reflectometry is the study of an object using reflected light. This experimental technique can be used to measure the thickness of a thin film. The idea of running the two experimental technique parallel at CHESS was to monitor the thin films in-situ giving us the ability to explore different solvent vapour annealing(SVA) protocols and see how the structure changed during these. The thickness measurements done at CHESS using Spectroscopic Reflectometry were not successful since the software's thin film model and the reflectance data did not fit well. Since beam time is precious, this problem was to be investigated back at Roskilde University in between beam times.

Spectroscopic Reflectometry is not the only experimental technique available that can measure thin film thickness, there is Atomic force microscopy, Ellipsometry and X-ray reflectometry. Spectroscopic reflectometry has been chosen to complement

GISAXS because it can be used in-situ and used in harsh conditions. The size of the apparatus plays a huge role as the free space in a synchrotron hutch is limited. It is a primitive technique compared to the other techniques that use electromagnetic radiation, and it is important investigate how far this technique can be pushed.

This thesis has two purposes, it is a study of how best to use the third party apparatus called NanoCalc XR spectrometer and software made by the company Ocean Optics, (<https://oceanoptics.com/>) and an investigation into how the reflectance measurements change during the solvent vapour annealing of homopolymers and copolymers.

The first purpose provides a experimental fundament since the NanoCalc XR spectrometer and software will be used to investigate the thin films and this thesis will serve as an introduction to the apparatus and how light reflects and transmits through the thin film since the user manual for the spectrometer and software is lacking in an explanation of the theory behind the thin film modelling and fitting.

The second purpose is the investigate how the reflectance curves change during solvent vapour annealing and is it possible to infer what is happening to the thin film during this process. This will be usefully for experiments conducted at synchrotron sources as the promising swelling protocols can be used.

1.1 Research Question

What are the advantages and limitations when using optical spectral reflectance for determining the thickness of thin polymer films during solvent vapour annealing?
[NHB - Not too sure about this research question, i have not though about the advantages and limitations.]

What is the optimal modelling and fitting method for the optical spectral reflectance measurements and thickness determination of homopolymers deposited on thin films during solvent vapour annealing?

Can the same thickness determination be used on thin films with a nano scale structure such as the block-copolymer Polystyrene-b-Polyisoprene?

1.2 Structure of this thesis

The structure of this thesis is as follows. Chapter 2 will introduce the basic theory of light propagation through a vacuum and through a transparent medium. It will touch on the complex refractive index and the Fresnel equations used to model light reflecting and transmitting in the thin films. Chapter 3 will introduce the polymers,

creation of the thin films, the Nanocalc spectrometer and how the measurements are taken.

Chapter 2

Theory

[2],[3]

2.1 Electromagnetic Radiation

Electromagnetic radiation can be expressed as a one dimensional sinusoidal wave using either cos or sin:

$$\varphi = A \sin(\omega t - Kx + \delta), \quad (2.1)$$

where A is the wave amplitude, $K = \frac{2\pi}{\lambda}$ is the propagation number and λ is the wave length, angular frequency $\omega = 2\pi\nu$ where ν is the frequency, time t and initial phase δ . From electromagnetic theory, the radiation is composed of an electric field and magnetic field that are both perpendicular to the direction of propagation. Both fields can be expressed as one-dimension complex sinusoidal wave. A complex number can be expressed as $C = a + ib = Re(C) + iIm(C) = r \cos(\theta) + ir \sin(\theta)$. Using Eulers formula $\exp(i\theta) = \cos(\theta) + i \sin(\theta)$, the one dimension sinusoidal wave can be expressed as:

Find
out
last =

$$\varphi = A \cos(\omega t - Kx + \delta) = Re\{A \exp[i(\omega t - Kx + \delta)]\} = A \exp[i(\omega t - Kx + \delta)]. \quad (2.2)$$

The wave travels to the right if the phase is $(\omega t - Kx)$ and to the left if the phase is $(\omega t + Kx)$. Changing the order of the first two terms in the phase does not change the propagation of the wave, only the initial phase δ . The wave equation in equation 2.1 uses sin in the expression but the complex wave in equation 2.2 uses cos, it is the same representation of the wave just moved 2π in the positive direction. The electric field and magnetic field can be expressed as:

$$E = E_0 \exp[i(\omega t - Kx + \delta)] \quad (2.3)$$

$$B = B_0 \exp[i(\omega t - Kx + \delta)]. \quad (2.4)$$

The relationship between the electric field and magnetic field is given by $E = cB$, and can be derived using the Maxwell-Faraday equation and one dimension wave equations for the electric and magnetic field:

$$\frac{\partial E}{\partial x} = -\frac{\partial B}{\partial t} \quad (2.5)$$

$$E = E_0 \cos(Kx - \omega t) \quad (2.6)$$

$$B = B_0 \cos(Kx - \omega t). \quad (2.7)$$

Using the Maxwell-Faraday equation the following equation can be formed:

$$\frac{\partial E}{\partial x} = -\frac{\partial B}{\partial t} \quad (2.8)$$

$$-KE_0 \sin(Kx - \omega t) = -\omega B_0 \sin(Kx - \omega t) \quad (2.9)$$

$$E_0 = \frac{\omega}{K} B_0 \quad (2.10)$$

$$E_0 = sB_0. \quad (2.11)$$

The constant $\frac{\omega}{K}$ is expressed as the speed s of the light through a medium. In vacuum the speed is equal to the speed of light $s = c$, through a transparent medium the speed is equal to the speed of light divided by the refractive index of the medium $s = \frac{c}{n}$.

2.2 Refractive index

Light travelling from one medium to another will undergo change. The speed of the light and the wavelength will change, but not the frequency. The refractive index is a material constant which describes the change and is greater than or equal to one. The refractive index is defined as:

$$n \equiv \frac{c}{s}, \quad (2.12)$$

where c is the speed of light and s is the speed of light in the medium. The amplitude of the wave will decrease in the medium because the propagation number $K = \frac{2\pi n}{\lambda}$ increases:

$$E = E_0 \exp \left[i(\omega t - \frac{2\pi n}{\lambda} x + \delta) \right]. \quad (2.13)$$

The change in wavelength is $\lambda = \frac{\lambda_0}{n}$, where λ_0 is the wavelength before entering the medium. The medium can also absorb light, a term is added to the refractive index to correct this, and is called the extinction coefficient k . The complex refractive index is given:

$$N = n - ik. \quad (2.14)$$

Placing the complex refractive index into equation 2.13, it can be seen that the waves amplitude will decrease exponentially.

$$E = E_0 \exp \left[i(\omega t - \frac{2\pi N}{\lambda} x + \delta) \right] = E_0 \exp \left(-\frac{2\pi k}{\lambda} x \right) \exp \left[i(\omega t - \frac{2\pi n}{\lambda} x + \delta) \right] \quad (2.15)$$

It needs to be stated that if the phase of the wave is expressed as $(Kx - \omega t)$ and the complex refractive index is given by $N = n - ik$, the exponentially factor will be positive which is incorrect. If the phase of the wave is expressed as $(Kx - \omega t)$ the complex refractive index must be defined as $N = n + ik$.

2.3 Reflectance and Transmittance

When light is reflected upon a surface at an oblique angle, light is reflected and transmitted. The electric field of light is grouped into two oscillation directions which can be defined by two planes, the parallel plane p and the perpendicular plane s. The same applies for the magnetic field of light. The parallel plane is defined by the incident and reflected light and the perpendicular plane is perpendicular to the parallel plane. Theory of light regards the two oscillation directions as the p-polarisation and s-polarisation. The reflectance of both p-polarisation and s-polarisation are defined by the ratio of reflected light intensity by the incident light intensity.

$$R_p \equiv \frac{I_{r,p}}{I_{i,p}} = \frac{|E_{r,p}|^2}{|E_{i,p}|^2} = |r_p|^2 \quad R_s \equiv \frac{I_{r,s}}{I_{i,s}} = \frac{|E_{r,s}|^2}{|E_{i,s}|^2} = |r_s|^2 \quad (2.16)$$

The transmittance can also be expressed using the intensity ratio, $I = N |E|^2$ and the ratio cross-sectional area for the transmitted and incident ray.

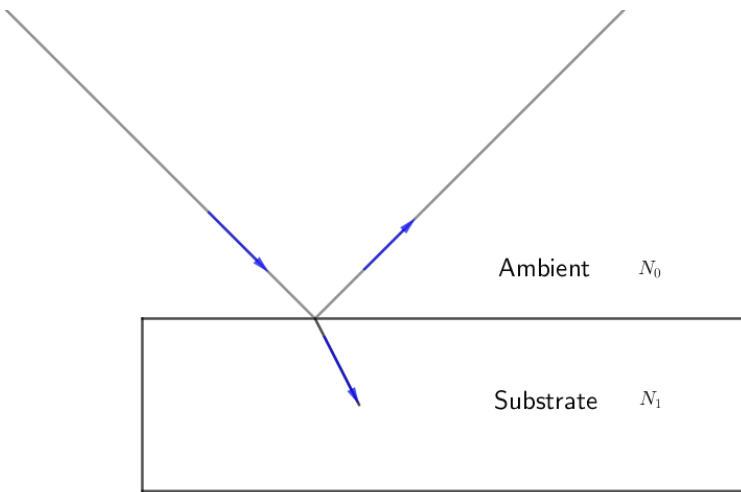


Figure 2.1: The components in this model is an ambient and a substrate both having a refractive index, N_0 and N_1 respectively. Light strikes the substrate reflecting with the same incident angle and refracting into the substrate. Equation 2.31 describes the amplitude reflectance coefficient of a ambient and substrate model.

$$T_p \equiv \frac{I_{r,p} \cos(\theta_t)}{I_{i,p} \cos(\theta_i)} = \frac{N_t \cos(\theta_t)}{N_i \cos(\theta_i)} \frac{|E_{tp}|^2}{|E_{ip}|^2} = \frac{N_t \cos(\theta_t)}{N_i \cos(\theta_i)} |t_p|^2 \quad (2.17)$$

$$T_s \equiv \frac{I_{r,s} \cos(\theta_t)}{I_{i,s} \cos(\theta_i)} = \frac{N_t \cos(\theta_t)}{N_i \cos(\theta_i)} \frac{|E_{ts}|^2}{|E_{is}|^2} = \frac{N_t \cos(\theta_t)}{N_i \cos(\theta_i)} |t_s|^2 \quad (2.18)$$

(2.19)

When the extinction coefficient in the refractive index is zero, $k = 0$, the sum of the reflectance and transmittance is equal to one, $R + T = 1$. If the extinction coefficient is greater than zero, $k > 0$, then the sum becomes less than one $R+T < 1$.

2.4 Fresnel equations for the ambient-substrate model

Light is reflected and transmitted at the interface of the ambient and substrate as seen in figure 2.1. The boundary conditions at the interface for the electric and magnetic field in the p-polarisation can be written as:

Need
to
under-
stand
why
B-field
is true

$$E_{i,p} \cos(\theta_i) = E_{t,p} \cos(\theta_t) + E_{r,p} \cos(\theta_r) \quad (2.20)$$

$$\implies E_{t,p} \cos(\theta_t) = E_{i,p} \cos(\theta_i) - E_{r,p} \cos(\theta_r) \quad (2.21)$$

$$B_{i,p} + B_{r,p} = B_{t,p}. \quad (2.22)$$

The subscripts of the electric and magnetic field denote the incident ray i , reflected ray r and transmitted ray t in the p-polarisation p plane. The same boundary conditions for the s-polarisation can be expressed. This introduction to the Fresnel equations will use the p-polarisation light. The boundary conditions of the magnetic field need to be reformulated to express the electric field, this is done using the relation $E = sB$. The magnetic field boundary conditions equation 2.22 can be expressed as:

$$\frac{E_{i,p}}{s_i} + \frac{E_{i,p}}{s_i} = \frac{E_{t,p}}{s_t} \quad (2.23)$$

$$\frac{N_i}{c}(E_{i,p} + E_{r,p}) = \frac{N_t}{c}E_{t,p} \quad (2.24)$$

$$N_i(E_{i,p} + E_{r,p}) = N_t E_{t,p}. \quad (2.25)$$

Though the law of reflection the angle of incident is also the angle of reflection $\theta_i = \theta_r$, placing this into the electric field boundary conditions equation 2.21, the electric field and magnetic field can be expressed as:

$$(E_{i,p} - E_{r,p}) \cos(\theta_i) = E_{t,p} \cos(\theta_t) \quad (2.26)$$

$$\frac{N_i}{N_t}(E_{i,p} + E_{r,p}) = E_{t,p}. \quad (2.27)$$

Placing equation 2.27 into equation 2.26, the amplitude reflectance coefficient and the reflectance can be calculated for the ambient-substrate system:

$$E_{i,p} \cos(\theta_i) - E_{r,p} \cos(\theta_i) = \frac{N_i}{N_t}(E_{i,p} + E_{r,p}) \cos(\theta_t) \quad (2.28)$$

$$E_{i,p} \cos(\theta_i) - \frac{N_i}{N_t} E_{i,p} \cos(\theta_t) = \frac{N_i}{N_t} E_{r,p} \cos(\theta_t) + E_{r,p} \cos(\theta_i) \quad (2.29)$$

$$E_{i,p}(N_t \cos(\theta_i) - N_i \cos(\theta_t)) = E_{r,p}(N_i \cos(\theta_t) + N_t \cos(\theta_i)) \quad (2.30)$$

$$r_p = \frac{E_{r,p}}{E_{i,p}} = \frac{N_t \cos(\theta_i) - N_i \cos(\theta_t)}{N_i \cos(\theta_t) + N_t \cos(\theta_i)} \quad (2.31)$$

$$R_p = |r_p|^2. \quad (2.32)$$

The amplitude transmission coefficient and transmission can be equivalently formulated.

2.5 Fresnel equations for the ambient-thin film-substrate model

The light reflecting and transmitting in this system will interfere both constructive and destructively. To model the optical interference, the Fresnel equation for reflection will be used:

$$r_{jk,p} = \frac{N_k \cos(\theta_j) - N_j \cos(\theta_k)}{N_k \cos(\theta_j) + N_j \cos(\theta_k)} \quad r_{jk,s} = \frac{N_j \cos(\theta_j) - N_k \cos(\theta_k)}{N_j \cos(\theta_j) + N_k \cos(\theta_k)}. \quad (2.33)$$

The subscripts denote the reflection and transmission at definite interface. For example $r_{jk,p} = r_{01,p}$, denotes the reflection at the ambient-thin film interface. In the ambient-thin film-substrate model, light at the ambient-thin film interface will be both reflected and transmitted into the layer. The transmitted ray will then be reflected and transmitted at the thin film-substrate interface. The reflected and transmitted phenomenon will proceed through out the thin film. The change in phase at the interface is given by $\exp(-i\beta)$. Figure 2.2 represents the ambient-thin film-substrate model, this figure will be used to define the phase variation β .

The phase of the reflected ray will vary at the the ambient-thin film interface. This variation can be expressed as $K_0 \bar{AD}$, where $K_0 = \frac{2\pi N_0}{\lambda}$, is the propagation number in air. The phase variation of the transmitted ray is expressed as $K_1(\bar{AB} + \bar{BC})$, where $K_1 = \frac{2\pi N_1}{\lambda}$, is the propagation number in the thin film. The length difference can be denoted as $\bar{AB} + \bar{BC} - \bar{AD}$, thus the phase variation of this length difference is:

$$\alpha = \frac{2\pi N_1}{\lambda}(\bar{AB} + \bar{BC}) - \frac{2\pi N_0}{\lambda}\bar{AD}. \quad (2.34)$$

Using snells law, $\bar{AD} = \bar{AC} \sin(\theta_0)$ and $\bar{AC} = 2d_1 \tan(\theta_1)$ as seen from figure 2.2, this reduces \bar{AD} to:

$$\sin(\theta_0) = \frac{N_1}{N_0} \sin(\theta_1) \quad (2.35)$$

$$\bar{AD} = 2d_1 \frac{\sin(\theta_1)}{\cos(\theta_1)} \sin(\theta_0) \quad (2.36)$$

$$\implies \bar{AD} = 2d_1 \frac{\sin(\theta_1)^2}{\cos(\theta_1)} \frac{N_1}{N_0}. \quad (2.37)$$

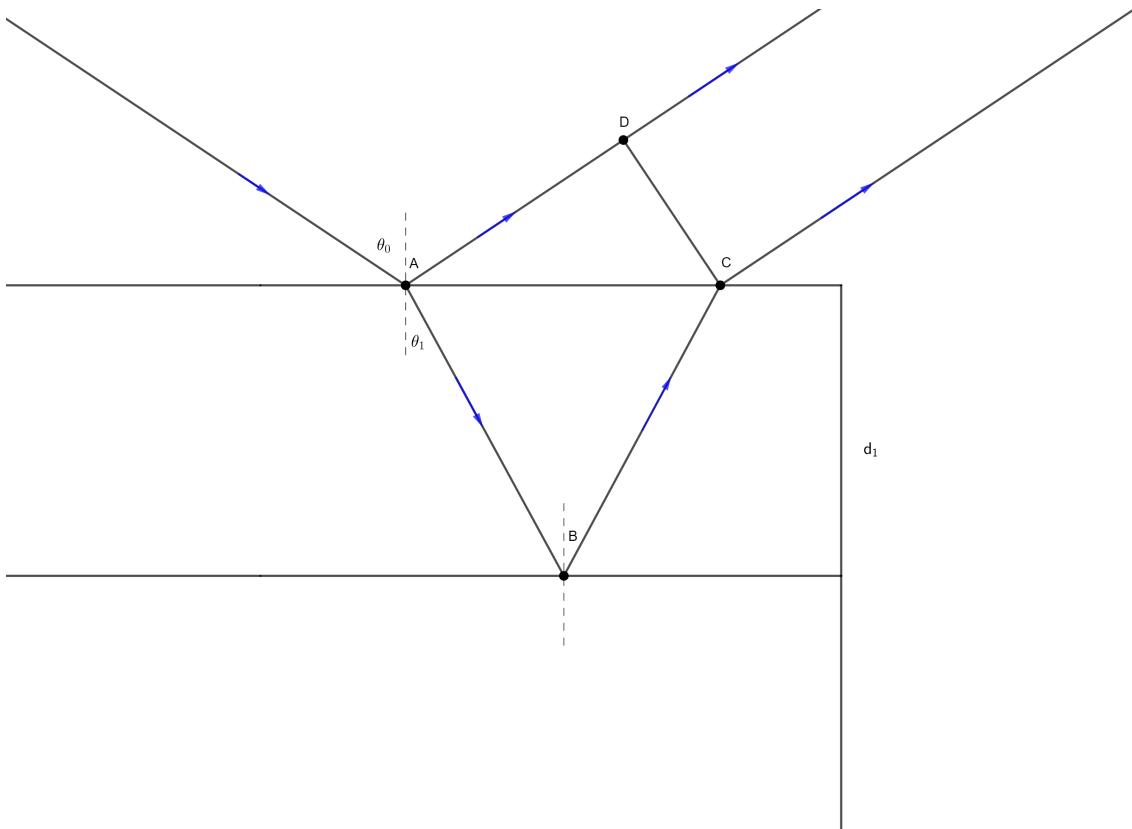


Figure 2.2: Light rays from the left will be reflected and transmitted at point A. The reflected light will experience a phase change at point A. The transmitted light will proceed to point B, where it will reflect undergoing a phase change then transmitting at point C. The phase difference between the primary and secondary ray can be calculated by $\alpha = K_1(\bar{AB} + \bar{BC}) - K_0(\bar{AD})$.

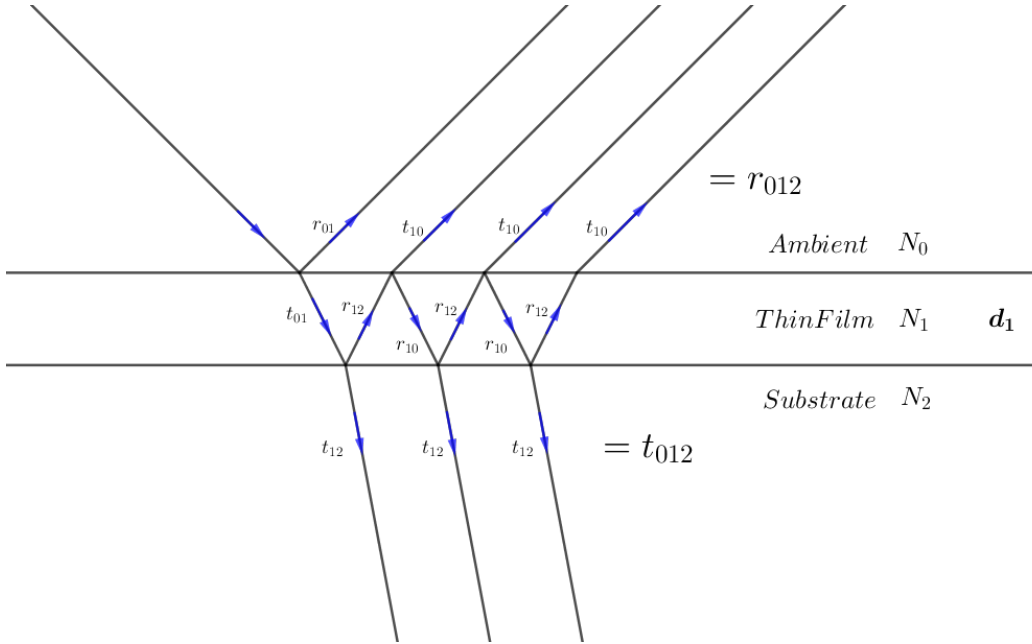


Figure 2.3: When light meets an interface, it reflects or transmits. Each light ray is name either reflection r or transmission t . Each reflected and transmitted ray is also indexed with two numbers, these denote at which interface the light was reflected or transmitted. A variation of phase happens to each reflected and transmitted rays at every interface. The phase variation at an interface can be expressed by the factor $\exp(-i\beta)$. The primary reflected beam is denoted as r_{01} , the second primary reflected beam is denoted $t_{01}r_{12}t_{10}\exp(-i2\beta)$. The reflection amplitude coefficient is the sum of reflected rays that exit the model. The transmission amplitude coefficient is the sum of the transmitted rays that continue into the substrate.

Inserting this into equation 2.34, and $\bar{AB} = \bar{BC} = \frac{d_1}{\cos(\theta_1)}$, as seen from figure 2.2, the equation is reduced to:

$$\alpha = \frac{2\pi N_1}{\lambda} \frac{2d_1}{\cos(\theta_1)} - \frac{2\pi N_0}{\lambda} \frac{2d_1 \sin(\theta_1)^2 N_1}{\cos(\theta_0) N_0} \quad (2.38)$$

$$= \frac{4d_1 \pi N_1}{\lambda} \left(\frac{1 - \sin(\theta_1)^2}{\cos(\theta_1)} \right) \quad (2.39)$$

$$= \frac{4d_1 \pi N_1}{\lambda} \cos(\theta_1). \quad (2.40)$$

α is the total phase difference of the transmitted beam thus the expression $\alpha = 2\beta$ must hold. β is called the film phase thickness and given as:

$$\beta = \frac{2\pi d_1}{\lambda} N_1 \cos(\theta_1). \quad (2.41)$$

Using figure 2.3 as a reference the amplitude reflection coefficient can be ex-

pressed as the sum of the reflected waves. The first time the ray meets the ambient-thin film interface, the ray will reflect and transmit. The reflected ray r_{01} can be calculated using equation 2.31. The transmitted ray will proceed to the next interface reflect back to the ambient-thin film interface and transmit, giving the second reflected wave in the sum expressed as $t_{01}r_{12}t_{10}\exp(-i2\beta)$. The factor $\exp(-i2\beta)$ comes from the phase difference due to the two interactions at the thin film-substrate interface and thin film-ambient interface. The phase difference factor can be collected and multiplied onto the expression since $\varphi = A \exp(i(\omega t - (Kx + 2\beta) + \delta)) = A \exp(i(\omega t - (Kx) + \delta)) \exp(-i2\beta)$. The total amplitude reflection coefficient can be expressed:

$$r_{012} = r_{01} + t_{01}t_{10}r_{12}\exp(-i2\beta) + t_{01}t_{10}r_{10}r_{12}^2\exp(-i4\beta) + t_{01}t_{10}r_{10}^2r_{12}^3\exp(-i6\beta) + \dots \quad (2.42)$$

The amplitude reflection coefficient becomes an infinite geometric series which can be reduced using $y = \frac{a}{(1-r)}$, leading to the coefficient being rewritten to:

$$r_{012} = r_{01} + \frac{t_{01}t_{10}r_{12}\exp(-i2\beta)}{1 - r_{10}r_{12}\exp(-i2\beta)}. \quad (2.43)$$

The equation 2.43 can be reduced to a more simple equation using $r_{10} = -r_{01}$ and $t_{01}t_{10} = 1 - r_{01}^2$:

$$r_{012} = \frac{r_{01} + r_{12}\exp(-i2\beta)}{1 + r_{01}r_{12}\exp(-i2\beta)}. \quad (2.44)$$

The following Fresnel equation, reflectance and Snell's law for this model are expressed as:

$$r_{012,p} = \frac{r_{01,p} + r_{12,p}\exp(-i2\beta)}{1 + r_{01,p}r_{12,p}\exp(-i2\beta)} \quad r_{012,s} = \frac{r_{01,s} + r_{12,s}\exp(-i2\beta)}{1 + r_{01,s}r_{12,s}\exp(-i2\beta)} \quad (2.45)$$

$$R_p = |r_{012,p}|^2 \quad R_s = |r_{012,s}|^2 \quad (2.46)$$

$$N_0 \sin(\theta_0) = N_1 \sin(\theta_1) = N_2 \sin(\theta_2). \quad (2.47)$$

2.6 Fresnel equations for a multilayer model

In the previous sections, the Fresnel equations for two different models were evaluated. The Fresnel equations for a multilayer model is an amalgamation of the

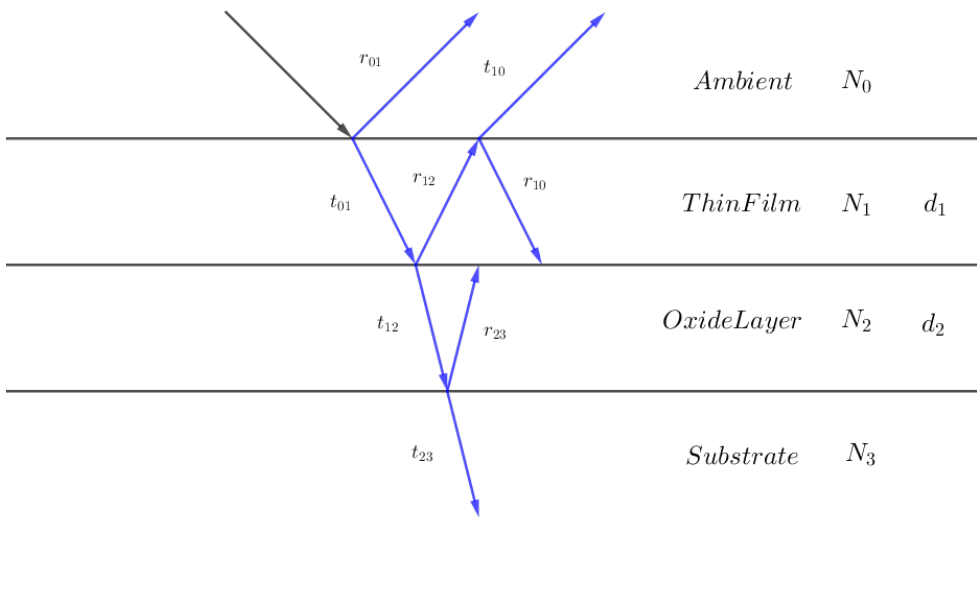


Figure 2.4: The model consists of the ambient, first thin film layer, second thin film layer and substrate. Each layer has a refractive index associated to it and both thin films have a thickness d_1 and d_2 respectively.

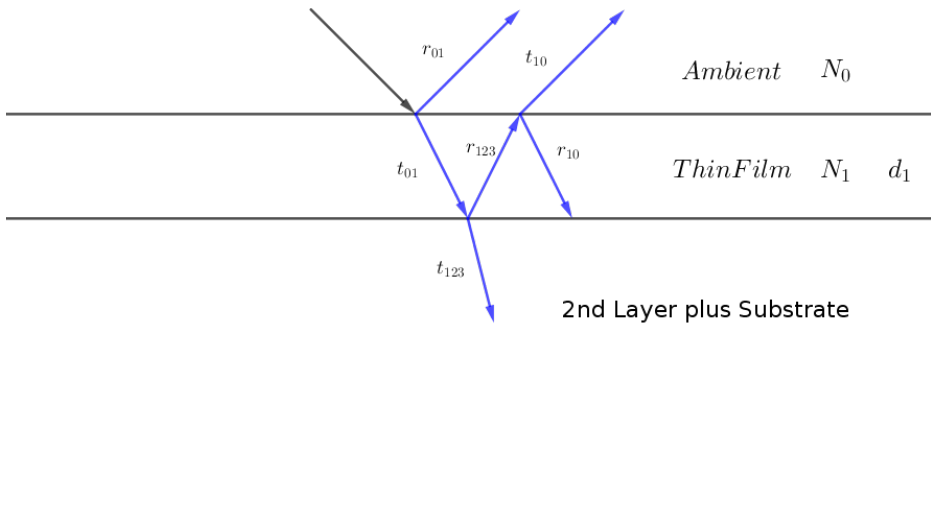


Figure 2.5: The model consists of the ambient, first thin film layer and second thin film layer plus substrate. The second thin film layer and substrate layer has been grouped together because r_{123} and t_{123} has been calculated the model seen in figure 2.4 and r_{0123} and t_{0123} can easily be calculated from this model. The ambient and first thin film layer have a refractive index and the first thin film layer has a thickness d_1 .

previous models. The reflection amplitude coefficient r_{123} for the multilayer model seen in the figure 2.4 with an ambient, two layers and a substrate can be calculated using equation 2.44. These equations produce the following expressions:

$$r_{123} = \frac{r_{12} + r_{23} \exp(-i2\beta_2)}{1 + r_{12}r_{23} \exp(-i2\beta_2)}. \quad (2.48)$$

β_2 is the phase variation in the second thin film layer with thickness d_2 . This is given as $\beta_2 = \frac{2\pi d_2 N_2 \cos(\theta_2)}{\lambda}$. The substrate and the layer on top of the substrate can be considered as one layer as seen in figure 2.5, thus the reflection amplitude coefficient and transmission amplitude coefficient is expressed as:

$$r_{0123} = \frac{r_{01} + r_{123} \exp(-i2\beta_1)}{1 + r_{01}r_{123} \exp(-i2\beta_1)}. \quad (2.49)$$

Inserting r_{123} into equations 2.49 gives the expanded Fresnel equation for this multilayer model:

$$r_{0123} = \frac{r_{01} + r_{12} \exp(-i2\beta_1) + [r_{01}r_{12} + \exp(-i2\beta_1)]r_{23} \exp(-i2\beta_2)}{1 + r_{01}r_{12} \exp(-i2\beta_1) + [r_{12} + r_{01} \exp(-i2\beta_1)]r_{23} \exp(-i2\beta_2)}. \quad (2.50)$$

Chapter 3

Experimental method

3.1 Polymers

Polymers are long chains of molecular units called mers, linked together by covalent bonds. Polymers are both found in biological system and synthesised by chemists. Polymers are described by their properties such as its chemistry, stereochemistry, architecture and what phase it is in [4]. A polymers chemistry is what the polymer is built of and with different structures, the polymers display different properties. Homopolymers are polymers built of one type of mer, where block copolymers are built up of two types of mers, an A and B. The different properties of the polymer is also dependant on how the repeating molecular units are bonded together, this is called the polymers stereochemistry, for example a block copolymer can be structured as a long chain of the A polymers bonded to a long chain of the B polymer. Polymers can be polar and non-polar due to the valence electron preferring one element from another. The polymers architecture describes the general structure of the polymer, which can be linear, branched or cross-linked. Linear polymers are long chains of monomers with bonds that are rigid to a certain degree, and cannot rotate freely, and are normally strong structures. Branched polymers are long chains with side chains attached to the main chain. These side chains can be comprised of monomers and reactive groups. Branched polymers are normally more softer and less crystalline than linear polymers. Cross-linked polymers are two or more side chains joined together forming a loose two dimensional network. Cross-linked polymers are more rigid and burn rather than melt when heated.

The architecture of a polymer can also be expressed with the degree of polymerisation, N , which characterises the average number of mers units in the chain. It is defined as:

$$N = \frac{\bar{M}_n}{\bar{m}}, \quad (3.1)$$

where \bar{M}_n is the number average molecular weight and \bar{m} is the mer molecular weight. The polymerisation of a block co polymer is the sum of the individual block polymerisation, $N = N_A + N_B$. The number average molecular weight is defined as:

$$\bar{M}_n = \frac{\sum N_i M_i}{\sum N_i} = \sum x_i M_i, \quad (3.2)$$

where $x_i = \frac{N_i}{\sum N_i}$ is the fraction of the number of chains with a corresponding size range i and M_i is mean molecular weight in the size range i . The weight average molecular weight for a polymer is defined as:

$$\bar{M}_w = \frac{\sum N_i M_i^2}{\sum N_i M_i}, \quad (3.3)$$

where N_i is the number of polymers with weight M_i . There is a dispersion of different polymer sizes in a solution, this dispersion is called the polydispersion index of the polymer and is expressed as:

$$PDI = \frac{\bar{M}_w}{\bar{M}_n}, \quad (3.4)$$

where \bar{M}_w is the weight average molecular weight and \bar{M}_n is the number average molecular weight [5].

The block co polymers can be further described by the volume fraction f that the different blocks take up and be the Flory-Huggins interaction parameter χ which describes the degree of incompatibility between the two polymers. The volume fraction of A and B blocks are respectively:

$$f_A = \frac{V_A}{V_{total}} \quad f_B = \frac{V_B}{V_{total}}. \quad (3.5)$$

The Flory-Huggins interaction parameter is determine experimentally and expressed as:

$$\chi(T) = \frac{\chi_H}{T} + \chi_S, \quad (3.6)$$

where χ_H is due to enthalpy and χ_S is due to entropy. Chemically dissimilar polymers tend to display a larger χ value than chemically similar,[6][7].

The polymers can also be in a physical state at a given temperature. The chemistry and architecture defines at what temperature the polymer undergoes a phase transition. A polymer can melt and transition into a liquid, which is often very viscous with viscoelastic properties. A polymer has trouble crystallising, polymers

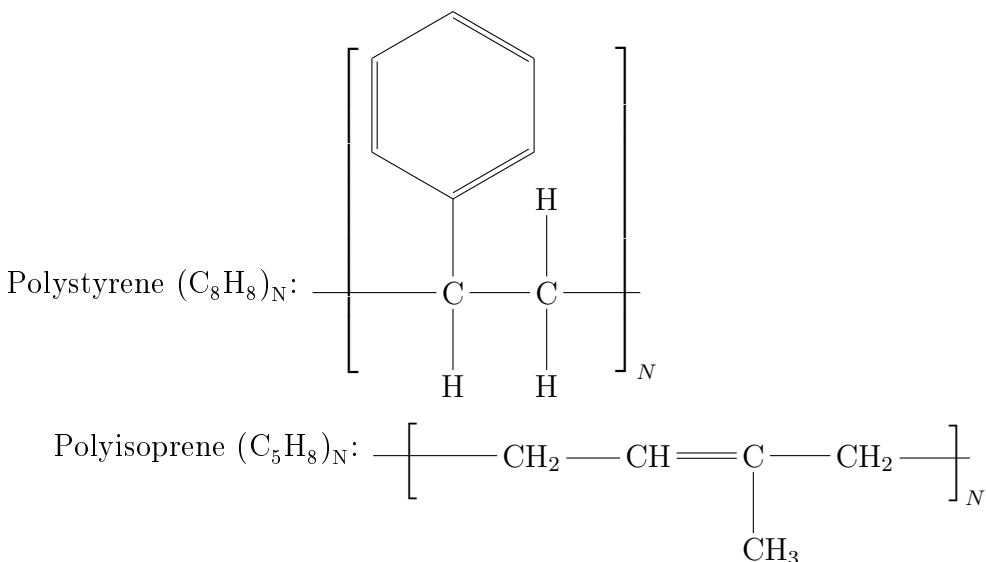
are most often in a glassy phase below the glass transition temperature T_g , a glassy phase is described as amorphous since the structure resembles both a liquid and a solid. A polymer can crystallise but the crystallisation is not complete because of the polymers architecture. This is called a semi-crystalline state where the polymer has regions behaving liquid like and glass like. And lastly a polymer can be in a liquid crystalline state which involves rigid polymers forming layers [8].

Micro-phase segregation of block copolymers is seen and understood as a thermodynamic process, in which the blocks of the polymer have a thermodynamic incompatibility described by Flory-Huggins interaction parameter χ_{AB} , which creates a nanoscale structure. The covalent bond between block A and block B prevent macro-phase separation, and micro-phase segregation occurs. This leads to the application of block copolymers as self-assembling structures that can be created on a surface and used for nanoscale devices. The applications span across a multitude of disciplines such as separation membranes, nanofluidics, photonics and biological scaffolds. The block copolymers self-assembling properties depend on the mobility of the polymer chains before structural reorganisation can proceed. This is normally done by thermal treatments above the polymers glass transition temperature T_g , but with high molar mass system long annealing times are needed [9].

3.2 Polymers used in Solvent Vapour Annealing

In this section the homopolymers Polystyrene and Polyisoprene and the block copolymer Polystyrene-b-Polyisoprene properties will be presented.

3.2.1 Homopolymer Chemistry



3.3 Polymer Considerations

Before commencing solvent vapour annealing some consideration is need into what polymers, what solvent and what substrate should be used. Polystyrene has been chosen as block A of the block copolymer and Polyisoprene chosen as block B. Polystyrene is in the glassy phase at room temperature, where polyisoprene is in a rubbery phase at room temperature. The morphology of the block can shed a light on how the vapour could interact with the blocks during solvent vapour annealing. The molar mass, polymerisation of both block, polydispersion index and the interaction parameter between the two block is helpful to understand what might happen during the solvent vapour annealing process. High molar mass systems are strongly segregated and take longer to come into equilibrium than a lower molar mass system.

3.3.1 Relevant values

Polymer Values			
	Polystyrene	Polyisoprene	PS-b-PI
T_g			
N			
N_A			
N_B			
f_A			
f_B			
\bar{M}_n			
\bar{M}_w			
PDI			
χ			

3.4 Spin Coating thin films

Spin coating is the deposition method used to fabricate the thin films used in this thesis. This is a wet method where a polymer is dissolved in a solution then deposited onto the semiconductor wafer, silicon wafer. The silicon wafer is rotated at a fixed low rpm to spread the polymer solution across the wafer. The rpm is increased spinning off the excess solution and will evaporate leaving a thin film with uniform thickness. This method is predicted by the following expression:

$$d = \left(\frac{\eta}{4\pi\rho\omega^2} \right)^{\frac{1}{2}} t^{-\frac{1}{2}}, \quad (3.7)$$

where d is the predicted thickness, η the viscosity coefficient of the polymer solution, ρ solution density, ω angular velocity of the spinning and t is the spinning time [8]. The spin coated block copolymers show defect-rich morphologies due to fast evaporation of the solvent and the polymers being in a thermal non-equilibrium [10].

3.5 Spectrometer Setup

The experimental setup is comprised of a NanoCalc XR and a Halogen light source(HL-2000-FHSA) seen in figure 3.2, which can produce wavelengths of 360 nm to 2400 nm. When the samples are being measured they are either placed on the ocean optics single point stage seen in figure 3.3 or in the test chamber seen in figure 3.4 made by the RUC workshop/machinists for x-ray scattering experiments. The NanoCalc is comprised of a spectrometer and an internal light source as seen in the figure 3.5, which can produce wavelengths of 250 nm to 1050 nm and measure thicknesses of 10 nm to 100 μm . The NanoCalc XR is connected to a computer where the NanoCalc software is installed and operated. For the experiments the halogen light source is used since it has a larger output power then the internal light source of the NanoCalc XR. The larger intensity output is need when performing experiments in the test chamber.

For experiments done in this thesis white light is produced in the light source(HL-2000-FHSA), which travels through optical fiber and strikes that sample. The reflected light travels back through the optical fiber and the intensity across every wavelength of the white light is collected in the spectrometer and is sent to software created by in house and saved to a file and analysed in MATLAB®.

3.6 Reflectance measurements in the NanoCalc spectrometer

The NanoCalc spectrometer measures three light intensities which will be called a measurement onwards. The three measurements are the dark measurement (dark), the reference measurement (ref) and the thin-film measurement (meas). The dark measurement is the amount of light received by the optical fiber from external sources. The reference measurement is the amount of light reflected from a blank

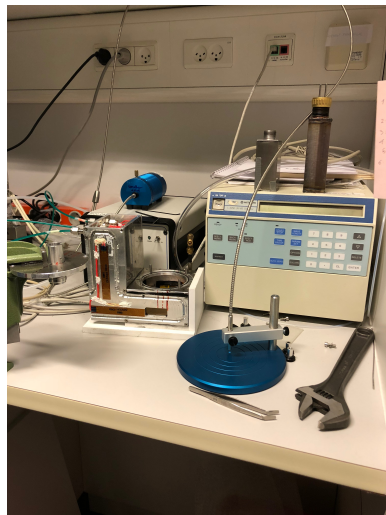


Figure 3.1: SVA experiment area

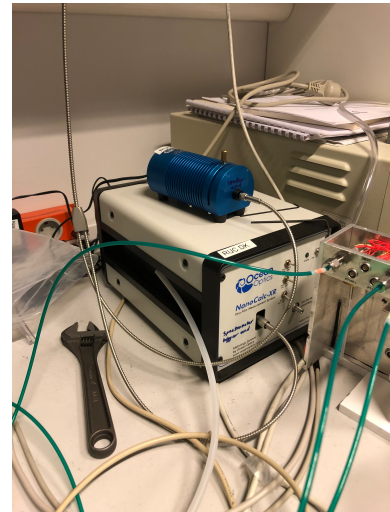


Figure 3.2: NanoCalc XR and a Halogen light source(HL-2000-FHSA)

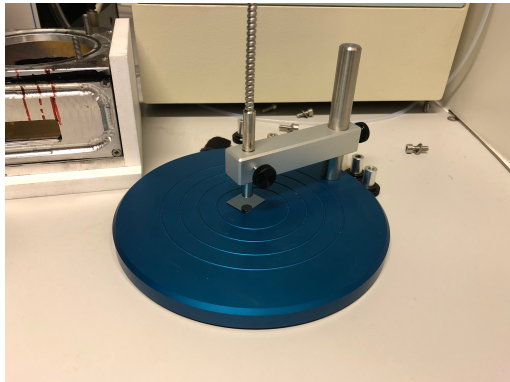


Figure 3.3: Single point stage

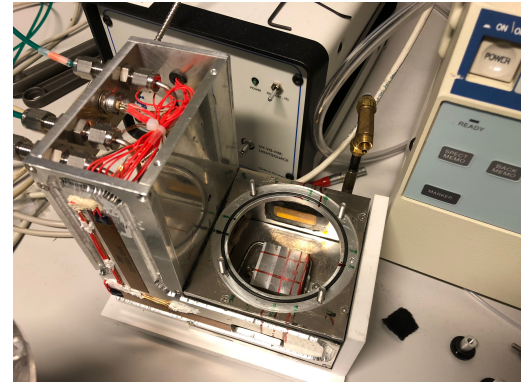


Figure 3.4: SVA experiment chamber minus lid

silicon wafer and the thin film measurement is the amount of light reflected from the sample. From chapter 2.3, the reflectance of a sample can be expressed as :

$$R_{sample} = \frac{I_{sample}}{I_{incident}}. \quad (3.8)$$

The spectrometer does not measure the intensity of the incident light, therefore the reflectance of the substrate is used to isolate the incident light intensity and inserted into equation 3.8. The reflectance of the substrate is used because it is easily calculated using the Fresnel equations as described in chapter 2.4.

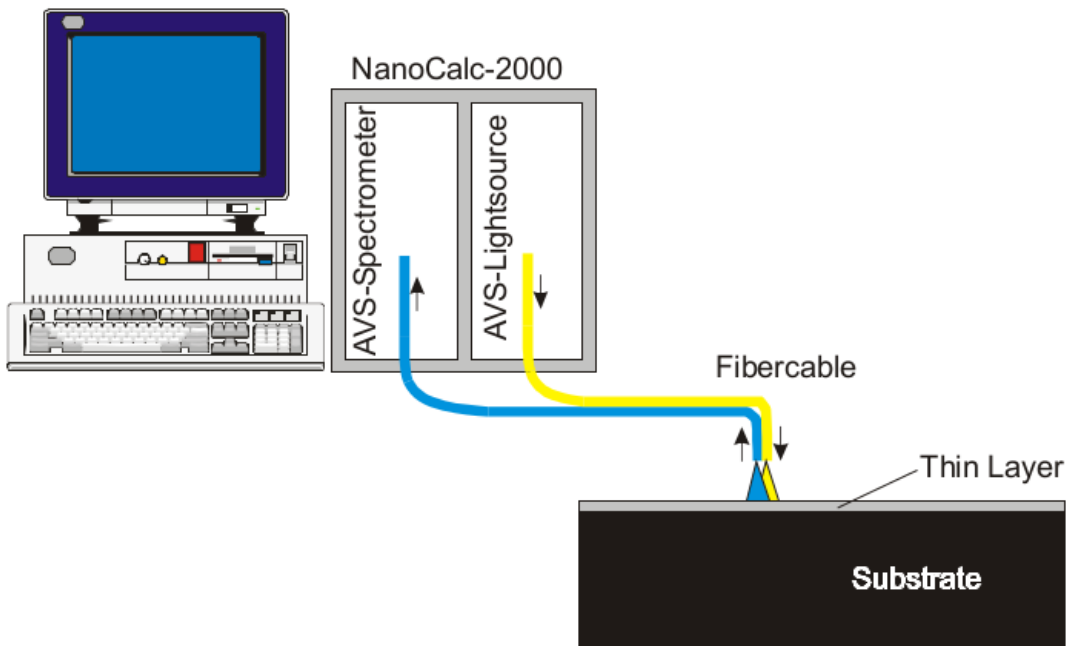


Figure 3.5: This figure describes the NanoCalc set-up and has been taken from [11]. Light from a light source travels down the optical fiber illuminating the sample. The reflected light is collected by the optical fiber and analysed in the spectrometer. The spectrometer is connected to the computer by USB and the data is stored, modelled and manipulated through the NanoCalc software.

$$R_{ref} = \frac{I_{ref}}{I_{incident}} \quad (3.9)$$

$$\implies I_{incident} = \frac{I_{ref}}{R_{ref}}. \quad (3.10)$$

Inserting equation 3.10 in equation 3.8, the reflectance for the sample is expressed without the incident light intensity as:

$$R_{sample} = \frac{I_{sample}}{I_{ref}} \cdot R_{ref}. \quad (3.11)$$

The reflectance of the sample is given as:

$$Reflectance = \frac{Meas - Dark}{Ref - Dark} \cdot R_{sub}. \quad (3.12)$$

This is the same expression given in the NanoCalc spectrometer manual [11]. Through reproduction of the data and curves given by the NanoCalc spectrometer, i can deduce that the reference measurement has already had the dark measurement subtracted, giving the following reflectance expression:

$$Reflectance = \frac{Meas - Dark}{Ref} \cdot R_{sub}. \quad (3.13)$$

Placing equation 3.13 equal to the reflectance equations using the Fresnel equations from chapters 2.4, 2.5 and 2.6, the NanoCalc spectrometer software can fit a thickness of the sample.

3.7 Reflectance measurement protocol

In this section the experimental protocol for both taking measurements without the optics and with the optics are given. The halogen light source has been turned on 30 minutes prior to taking the measurements and the thin films have had 30 minutes to climatise to room temperature. The protocol will be formulated in steps.

3.7.1 Without Optics

1. Take a continuous reference measurement and adjust the light intensity, such that the reference measurements maximum is 50% of the y-axis.
2. Clear the reference measurement.
3. Take the optic fiber and point it away from anything that can reflect light.
Take a dark measurement.

4. Place the optic fiber into ocean optics single point stage. The optic fiber is positioned 4mm above the single point stage.
5. Place a blank silicon wafer under the optic fiber and take a reference measurement.
6. Save the dark and reference measurement.
7. Place a thin film under the optical fiber and take a measurement.

3.7.2 With Optics

1. Take a continuous dark measurement with the optic fiber with a dark cloth in the optics where the thin film would lie and adjust the light intensity, such that the dark measurements maximum is at 100% of the y-axis.
2. Clear the dark measurement.
3. Take the optics as a whole and point it away from anything that can reflect.
Take a dark measurement.
4. Place a blank silicon wafer into the test chamber and place the optics into the test chamber. Take a reference measurement.
5. Save the dark and reference measurement.
6. Take the optics off the test chamber, remove the blank silicon wafer and place in a thin film sample. Place the optics onto the test chamber. Take a measurement.

3.8 MATLAB® result fitting

450-900nm, MSE, Three parameters n0,n1,D1.

3.9 Bronkhorst mass flow meters

To regulate the solvent vapour annealing process, the experimental setup includes three Bronkhorst mass flow meters. This is important since controlling the vapour flow in different ways changes the structuring of the polymers when swelling. One EL-Flow select(F-201CV-500) with a flow capability for N_2 of 4 ml min^{-1} to 750 ml min^{-1} , or 400 SCCM (Standard centimetre cubed per minute at 1 atm and 273 K). Two

EL-Flow select(F-201CV-200) with a N_2 flow of 1.6 ml min^{-1} to 300 ml min^{-1} , or 200 SCCM (Standard centimetre cubed per minute at 1 atm and 273K) [12].

During the both swelling processes, the SCCM will be kept constant to 200 SCCM, with the assumption that the flowrate is constant through the system. When nitrogen flows through the bubbler and solvent the flowrate will change and thus the pressure in the SVA chamber will change.

3.10 Solvent Vapour Annealing Process

The solvent vapour annealing process is divided into two process, a swelling and a drying process. In the swelling process a dry polymer upon a wafer is placed into the annealing chamber and is subjected to nitrogen gas. Slowly nitrogen gas is decreased and nitrogen gas through a bubbler filled with a solvent, in this thesis toluene, is increased creating vapour in the annealing chamber. When performing SVA, a solvent is chosen that is either neutral or slightly selective towards one of the polymers in the block copolymer. Solvent uptake is also dependant on the physical state of the block copolymer and the block fraction volume. The thin film will swell due to thermodynamic driving forces associated with the entropy of mixing of vapour and polymer blocks. The swelling will continue until the chemical potential of the vapour and the solvent in the thin film is in equilibrium. A diffusion front will arise continuing through the thin film from the vapour interface through to the substrate. It is published that the vapour pressure is an important thin film thickness parameter and should be controlled throughout the annealing. The vapour pressure is dependant on the mass flow controller, temperature of the solvent and temperature of the annealing chamber. The time taken to fully swell is also dependant on how organised the dry thin film is before swelling, this leads to varying swelling time. In a solvent swollen state the mobility of the polymer chains increase and the polymer can move in the volume of the thin film. The molar mass of the polymer plays a role in the how fast the polymer self assembles and a equilibrium state may not be achieved during the swelling. In the drying step the nitrogen gas flow through the bubbler is decrease and the direct nitrogen gas flow is increased. The solvent in the thin film is evaporated and the rate in which the solvent evaporates has been seen to have an impact of the nanoscale structure, in effect of quenching an organised structure. It is documented that both fast and slow evaporation leads to organised structure in block copolymers. An ordering front forms in the thin film during the evaporation where the thin film show order closer to the vapour interface and as the front propagates through the film, order follows in its wake[9].

Structure characterisation is important during the stages of solvent vapour annealing, different experimental method illuminate different parameters. Spectral reflectometry used in this thesis will investigate how the thickness of the thin film evolves during SVA and shed light on how the refractive index for the ambient and thin film could evolve.

Chapter 4

Analysis

4.1 Nano-Calc Simulated Reflectance Curves

4.2 Day study

4.3 Ambient study

4.4 Polystyrene

4.5 Polyisoprene

4.6 Polystyrene-b-polyisoprene

Chapter 5

Bibliography

- [1] I. Levine. *Physical Chemistry*. McGraw-Hill, 1995.
- [2] H. Fujiwara. *Spectroscopic Ellipsometry: Principles and Applications*. Wiley, 2007.
- [3] H.G. Tompkins and J.N. Hilfiker. *Spectroscopic Ellipsometry: Practical Application to Thin Film Characterization*. Materials Characterization and Analysis Collection. Momentum Press, 2015.
- [4] R.A.L. Jones. *Soft Condensed Matter*. Oxford Master Series in Physics. OUP Oxford, 2002.
- [5] G.R. Strobl. *The Physics of Polymers: Concepts for Understanding Their Structures and Behavior*. Springer Berlin Heidelberg, 2007.
- [6] Frank S. Bates and Glenn Fredrickson. Block copolymer thermodynamics: Theory and experiment. *Annual review of physical chemistry*, 41:525–57, 10 1990.
- [7] Daniel J. Kozuch, Wenlin Zhang, and Scott T. Milner. Predicting the flory-huggins parameter for polymers with stiffness mismatch from molecular dynamics simulations. *Polymers*, 8(6), 2016.
- [8] M.C. Petty. *Molecular Electronics: From Principles to Practice*. Wiley Series in Materials for Electronic & Optoelectronic Applications. Wiley, 2008.
- [9] Christophe Sinturel, Marylène Vayer, Michael Morris, and Marc A. Hillmyer. Solvent vapor annealing of block polymer thin films. *Macromolecules*, 46(14):5399–5415, 2013.
- [10] Dorthe Posselt, Jianqi Zhang, Detlef-M. Smilgies, Anatoly V. Berezkin, Igor I. Potemkin, and Christine M. Papadakis. Restructuring in block copolymer thin

- films: In situ gisaxs investigations during solvent vapor annealing. *Progress in Polymer Science*, 66:80–115, 2017.
- [11] Ocean Optics. *NanoCalc Software Manual*, version 4 edition, 2014.
- [12] Bronkhorst. *El-Flow® select Brochure*. Available at <https://www.bronkhorst.com/products/gas-flow/el-flow-select/f-201cv/>.